Proceedings of the
International Conference on Mechanical Engineering and Renewable Energy 2019
(ICMERE2019) 11 – 13 December, 2019, Chittagong, Bangladesh

ICMERE2019-PI-091

NUMERICAL STUDY ON THE EFFECT OF MACH NUMBER AND ANGLE OF ATTACK ON SHOCK WAVE FORMATION IN TRANSIENT REGIME

Md. Mahmudul Hasan[1], Abdullah Al-Faruk[1]

[1,1] Department of Mechanical Engineering, Khulna University of Engineering & Technology (KUET), Bangladesh.
mahmudshikdar@gmail.com[1], alfaruk@me.kuet.ac.bd[2]

Abstract: *Nowadays, modern jet engines are designed to run in the transonic region. Although fighter and space aircrafts are able to achieve supersonic regions, most of the time they operate in the transonic region. Onset of shock wave is an important phenomenon in this region that increases the drag force rapidly and decreases the lift force. The study investigated the relation between the onset of shock on an ONERA wing with the Mach number and angle of attack. An ONERA M6 wing was used as the subject wing which is mainly a definitive CFD validation case for peripheral flows. The flow simulation was done on the ANSYS-Fluent using Spalart Allmaras Turbulence modeling. The increase of Mach number hastens the onset of shock and the positive increase of angle of attack increases the drag and lift and pushes the downstream shock wave further towards downstream. The Mach number for the onset of shock and the lift and drag force variation with angle of attack can be used to design maximum speed of an aircraft and the most acceptable wing profile.*

Keywords: Transonic flow, shock wave, Mach number, angle of attack, drag and lift coefficients.

INTRODUCTION

Transonic flow is the flow with the speed near to sound. Therefore the flow with Mach number ranging from 0.72 to 1.2 falls in this region [1]. It is one of the most investigated topics in the flight dynamics since 1930[2-10] because of the coefficient of pressure variation, inauguration of shock waves, turbulence boundary layer interaction etc. Transonic flow causes boundary separation resulting instabilities [11]. When the Mach number goes beyond 0.8, there is a rapid increase of drug due to the vicious shock waves. Nowadays, modern jet engines are designed to run in the transonic region. Subsonic airplanes, such as Boeing 777,747 are engineered to run at a Mach number of 0.85. Additionally Air bus A380 and Boeing 787 runs at the same Mach number and Boeing 747-8i runs with a Mach number of 0.86. The airplane Cessna Citatoin X+ runs with a Mach number of 0.95[12]. Thus, a large number of aircrafts operate in the transonic regime. Again, although fighter and space aircrafts care able to achieve supersonic regions, most of the time they operate in the transonic region. So the properties in this flow region is a matter of great interest. Within viscous flow regions, changes in the flow field occur in non-monotonic pattern and prompts surface instability, even in the absence of unstable boundary condition. In this manner, transonic streams must be represented with transient conditions and compressible Navier-Stokes conditions. ONERA Aerodynamics department designed an ONERA M6 wing in 1972. It had been designed by Bernard Monnerie and his aerodynamicist colleagues. As it was being designed on experimental geometry for reviewing high Reynolds number and three dimensional flows with some multi-faceted, complex flow circumstances [13], comparatively unpretentious geometry, complex flow physics, and accessibility of experimental data. It is a swept, semi span wing with no twist. It uses a symmetric airfoil using the ONERA D section [14]. Variation of aerodynamic characteristics such as variation of drag and lift force, inauguration of shock wave etc. are one of the most important phenomenon in this region. It can vary with the flight condition such as operating Mach number, angle of attack etc.

FLOW CHARACTERISTICS

As the variation of aerodynamic characteristics with the variation of operating condition is a major concern here, flow characteristics include a varying Mach number region and a varying angle of attack. The Mach number was increased at a rate of 0.1 from Mach number 0.8395(~0.84) to 0.90 and angle of attack was increased at a rate of 0.2 ranging from 3.06° to 4.26°. No angle of sideslip was imposed. The Reynolds number was selected to be 11.72 E+06.

The wing itself has the following dimensions shown in table 1:

Table 1: Wing Specifications.

Specification	Dimension
Wing root chord	0.67 ft.
Wing tip chord	0.38 ft.
Taper ratio	0.562
Half wing span	1 ft.
Leading edge sweep angle	30°
Trailing edge sweep angle	15.8°
Aspect ratio	3.8
Wing Twist	No

COMPUTATIONAL SETUP

i . Geometry Generation

The coordinate for ONERA OA206 airfoil was found from the airfoiltools.com. The coordinate has been obtained for 100 points on the upper and lower surface of airfoil. From the airfoil, the wing geometry was designed in SOLIDWORKS 2018. Then the wing was imported to ANSYS DesignModeler. The wing is shown below in Figure 1:

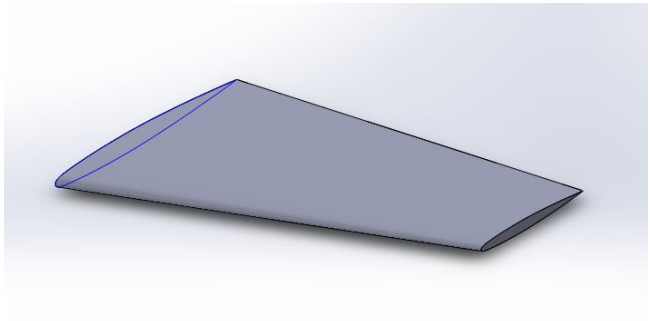

Figure 1: ONERA M6 half wing span.

As shown in figure 2, flow domain was created with dour named boundaries – inlet, outlet, near side and far side. The wing face was split into four faces for better visualization in the leading and trailing edges.

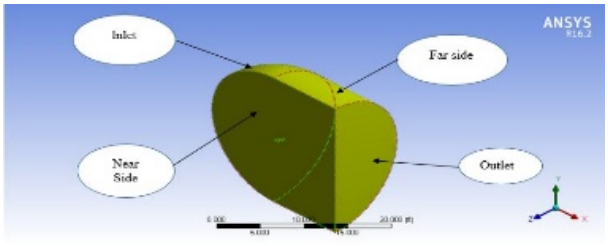

Figure 2: Flow domain of transonic flow over a 3D wing.

ii . Meshing

The geometry was meshed using ANSYS-Meshing component of Workbench. Unstructured triangular mesh was primarily generated in the flow domain. This procedure includes a body of influence to get denser mesh near the wing as shown in figure 3 a). To capture the boundary, some inflation layers were made near the surface of the wing as shown in figure 3 b). Inflation layer gives structured mesh. That gives better result in computational analysis than the unstructured one. Leading edge and trailing edge of wing require denser meshing than other parts of the wing to visualize the interaction between shock and boundary layers.

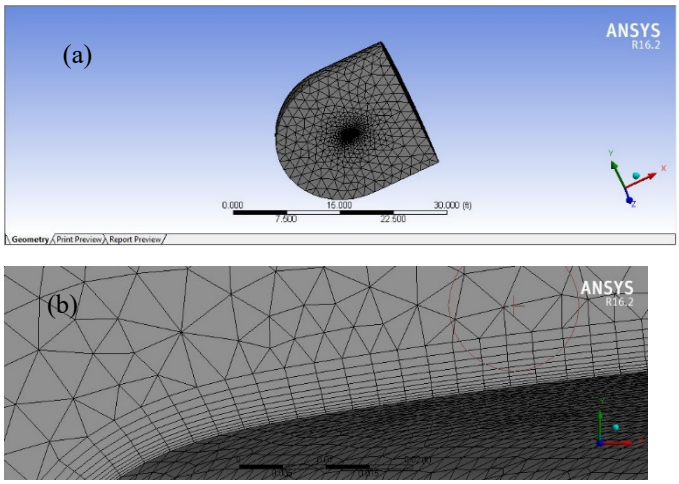

Figure 3: a) Meshing with denser mesh in the body of influence. b) Structured mesh in the inflation region

A total 627523 nodes were used for the mesh analysis. That covers up 1928350 elements. Total 10 inflation layers were used and maximum thickness of 0.006 ft. were used.

iii . Boundary Conditions

For the sake of validation, the boundary conditions are set as same as the boundary conditions flow field conditions of Test 2308 of Reference [15]. Boundary conditions are shown in table 2:

Table 2: Boundary Conditions.

Boundary name	Type	Condition
Near side	Symmetry	Symmetry with respect to boundary
Wing Wing tip	Wall	V=0
Far side Inlet Outlet	Pressure far field	Pressure = 45.829 psig Temperature = 460 R Mach number = 0.8395 - 0.89 Angle of attack = 3.06° – 4.26°

The fluid properties are also an important factor in solving the problem. The density of the fluid was set to be of an ideal gas. Specific heat and thermal conductivity were set as 0.240388 btu/lb-r and 0.01398601 btu/h-ft-r, respectively. The viscosity of the fluid was taken as 1.09329 e-5 lbm/ft-s.

iv. Solver, Models and Solution Method:

Pressure based solver was used with absolute velocity formation and steady state condition. The energy equation was involved and for turbulence modeling Spalart Allmaras equation was used. This Spalart-Allmaras model was designed specifically for aerospace applications involving wall-bounded flows and has been shown to give good results for boundary layers subjected to adverse pressure gradients [16]. In the solution method, pressure velocity coupled scheme was used and for quick convergence, pseudo transient approach was used with high order term relaxation.

VERIFICATION AND VALIDATION OF CFD RESULTS

This case involves the flow over the ONERA M6 wing. It was tested in a wind tunnel at transonic Mach numbers (0.7, 0.84, 0.88, and 0.92) and various angles-of-attack up to 6 degrees. The Reynolds numbers were about 12 million based on the mean aerodynamic chord. The wind tunnel tests are documented by Schmitt and Charpin in the AGARD Report AR-138 published in 1979 [15].

a.Verification

The result was verified for the Mach number 0.8395 and at an angle of attack of 3.06°. NASA CFD results from are available for verification of C_L and C_D CFD results [17]. Table 3 shows a comparison of the present Fluent CFD results with the NASA CFD software results.

Table 3: Verification of drag and lift force co efficient

	Lift Coefficient, C_L	Drag Coefficient, C_D	% Error	
			C_D	C_L
NASA CFD	0.1410	0.0088	-	-
Fluent result	0.1311	0.0094	7.02%	6.82%

b. Validation

A polyline was drawn at a span wise distance of 0.2 ft. to validate the result by comparing pressure coefficient with Data files for pressure coefficients obtained from the experiment by Schmitt and Charpin (1979) [15]. The comparison results is shown in figure 5:

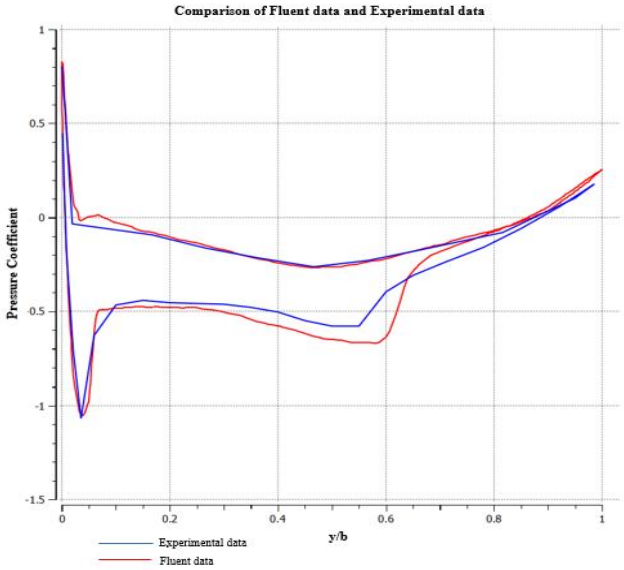

Figure 5: Comparison of Experimental data with fluent data.

The graph represents the variation of pressure coefficient at different sections of the wing along chord line at a distance of 0.2 ft. from the wing root. The blue line is for the experimental data obtained by Schmitt and Charpin (1979) [15]. The red line represents the fluent data obtained by the numerical analysis. From the graph it can be seen that at the leading edge the deviation of these two lines are very small. At about the middle of the chord a more deviated fluent data line can be seen. The trailing edge pressure coefficients from the numerical analysis are greater than the data obtained from the experiment.

RESULTS

i. Variation of Drag and Lift Force with Mach number

It is seen that drag coefficient increases with the increase in the Mach number. It is also seen that the drag coefficient increases more likely with a linear relationship with the Mach number. The magnitude of increasing the drag coefficient with the Mach number almost maintain the same level from Mach number 0.84 to 0.89. But when the Mach number reaches 0.89, the slope of increase becomes steeper. For lift coefficient it is seen that with the increase of the Mach number the lift coefficient also increases. That increase is more substantial than the drag coefficient increase. But after the Mach number 0.89 the lift coefficient starts to decrease. More over the lift coefficient increase rate is less at the Mach number range from 0.87 to 0.89 than the lift coefficient increase rate at the Mach number range from 0.84 to 0.87. Thus, though lift coefficient increases more rapidly than the drag coefficient with the Mach number, the rate of increase decreases at higher Mach number. The result is shown graphically in Figure 6:

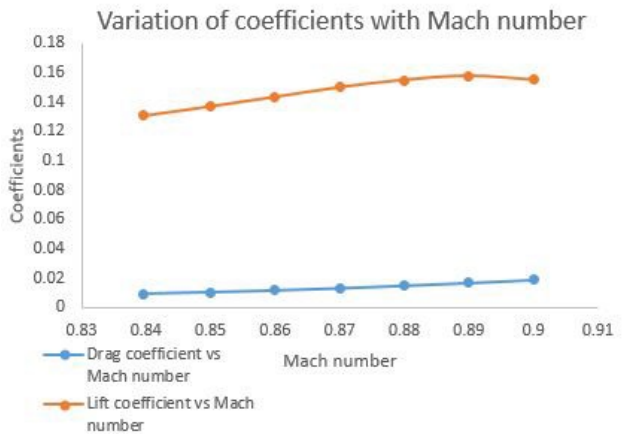

Figure 6: Variation of Drag and lift coefficient with Mach number.

ii . Onset of Shock with Variation of Mach number

It is seen that creation of shock wave hastens with the increase of Mach number. The upstream shock region expands with the increase in the Mach number. The shockwave at downstream moves further towards downstream with increase in the Mach number. This shows great agreement with research article from Alexander Kuzmin [18]. Onset of shock with variation in the Mach number is presented below:

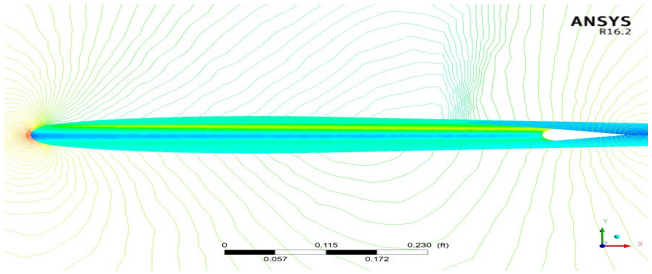

Figure 7: Shock creation at Mach number 0.8395

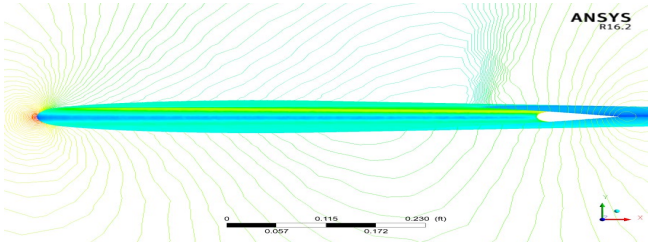

Figure 8: Shock creation at Mach number 0.85

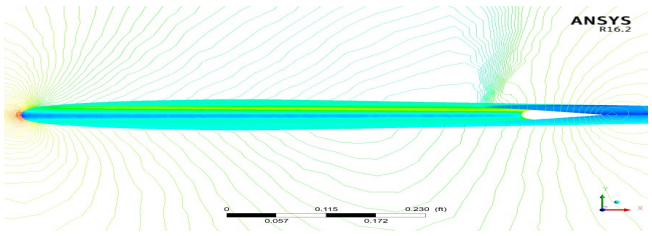

Figure 9: Shock creation at Mach number 0.86

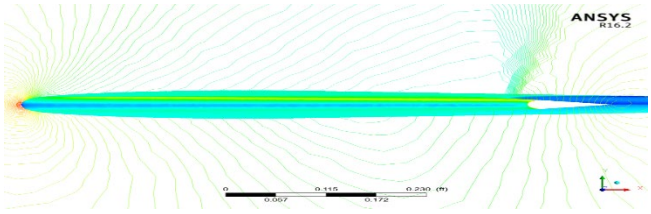

Figure 10: Shock creation at Mach number 0.87

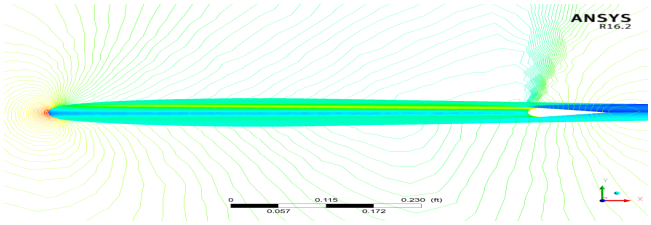

Figure 11: Shock creation at Mach number 0.88

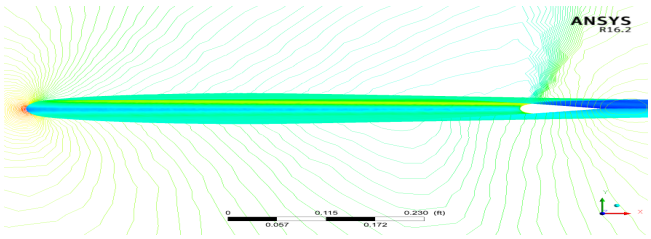

Figure 12: Shock creation at Mach number 0.89

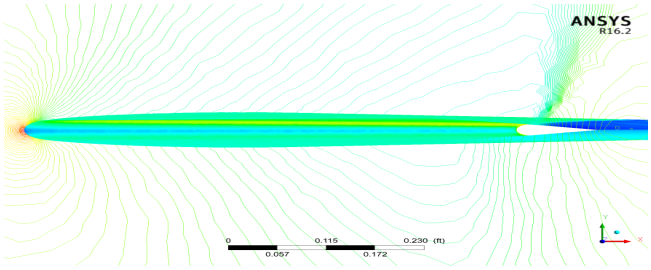

Figure 13: Shock creation at Mach number 0.90

iii . Variation of Drag and Lift Coefficient with Varying Angle of Attack

The drag and lift coefficient both increases with the increase of angle of attack. However, at the angle of attack ranging from 3.06° to 4.26°, lift coefficient increases more significantly than the drag co-efficient with the increase of the angle of attack at the Mach number 0.8395. Literally, the slope of the line representing the increase of drag coefficient with the increase of the Mach number is very low. Thus it can be said that increasing the angle of attack will increase the lift without a significant change in the drag.

The graphical representation is presented in figure 14:

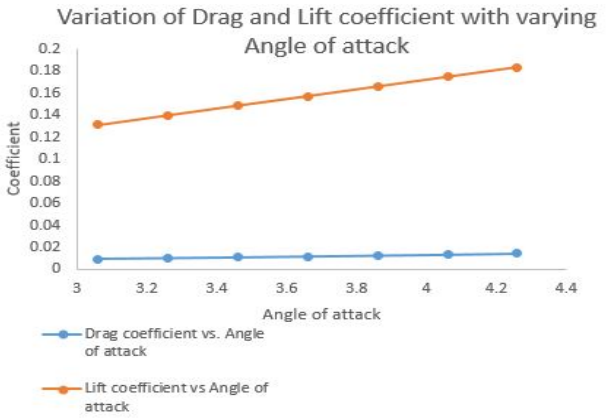

Figure 14: Variation of Drag and Lift coefficient with variation of angle of attack.

ⅳ. Onset of Shock with Variation of Angle of Attack

Shock wave at the downstream moves more towards downstream with the increase of the angle of attack. Thus it signifies the expansion of leading edge shock region with the increase of angle of attack. The position of shock wave at various angle of attack is shown below:

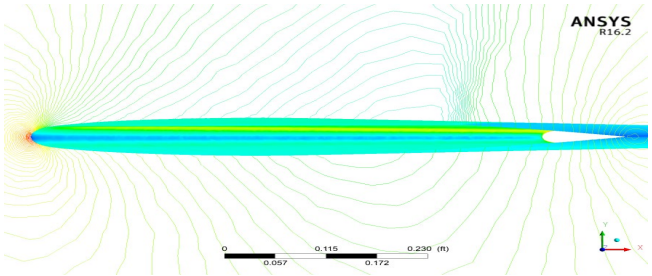

Figure 15: Shock creation at angle of attack 3.06°

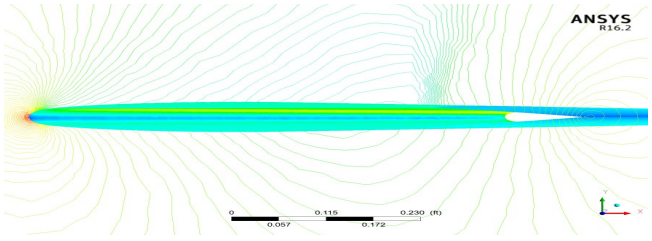

Figure 16: Shock creation at angle of attack 3.26°

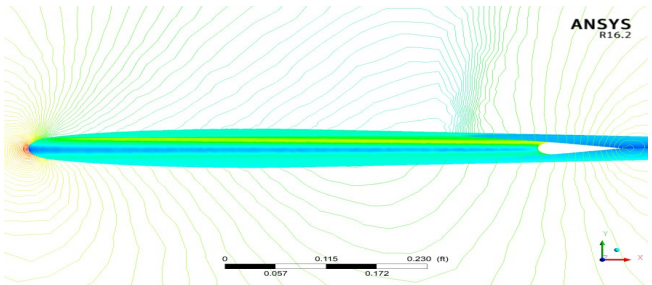

Figure 17: Shock creation at angle of attack 3.46°

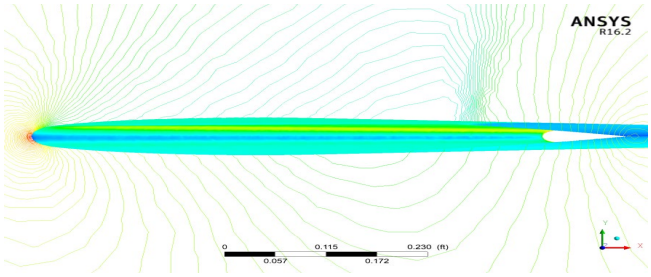

Figure 18: Shock creation at angle of attack 3.66°

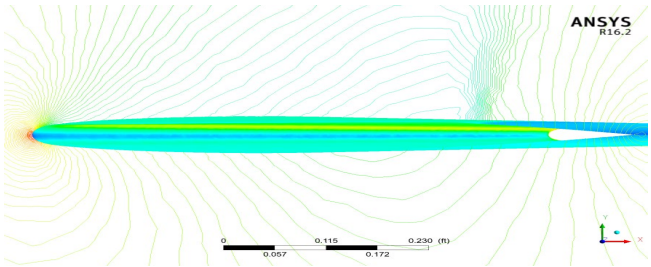

Figure 19: Shock creation at angle of attack 3.86°

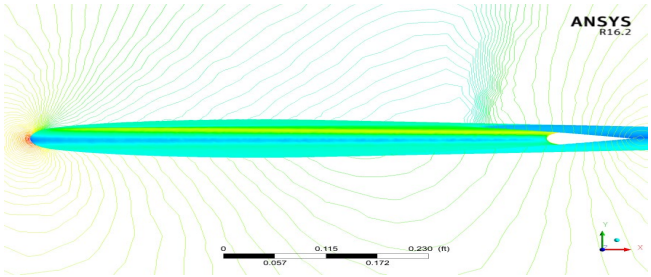

Figure 20: Shock creation at angle of attack 4.06°

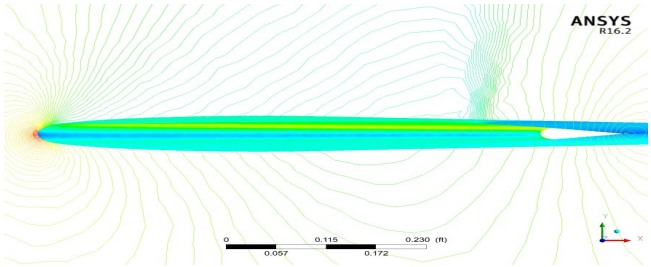

Figure 21: Shock creation at angle of attack 4.26°

CONCLUSION

The validation of the CFD result shows good agreement with the experimental data. The drag and lift coefficient both increases with the increase of Mach number and angle of attack. At very high Mach number in transonic regime, degradation of lift coefficient is noticed. The Mach number has a significant effect on the onset of shock. Also the change of angle of attack at smaller range put much emphasis on it.

REFERENCES

1. https://www.skybrary.aero/index.php/Transonic_Flight (13-09-2019)
2. Antony Jameson “Numerical Calculation of the Three Dimensional Transonic Flow over a Yawed Wing”, 1973
3. Antony Jameson, “Iterative Solution of Transonic Flows over Airfoils and Wings, Including Flows at Mach 1”, Communications on Pure and Applied Mathematics, Vol. XXVII, 283-309 ,1974
4. Theodore G. Ayers, James B. Hallissy, “Historical Background and Design Evolution of the Transonic Aircraft Technology Supercritical Wing”, NASA Technical Memorandum 81356, August 1981.
5. A. Jameson, T.J. Baker and N.P. Weatherill , “ Calculation of Inviscid Transonic Flow over a Complete Aircraft”, AIAA- 86-0103, 1986
6. V. N. Vatsa, B. W. Wedan, “Navier-Stokes Solutions for Transonic Flow over a Wing Mounted in a Tunnel”, AIAA-88-010,1988
7. Antony Jameson and D. A. Caughey “A Finite Volume for Transonic Potential Flow Calculations”, 2007
8. Naveed Durrani and Ning Qin “Comparison of RANS, DES and DDES results for ONERA M-6 Wing at transonic flow speed using an in-house parallel code.”, AIAA 2011-190, 2011
9. Eirikur Jonsson, Leifur Leifsson and Slawomir Koziel, “Aerodynamic Optimization of Wings by Space Mapping”, AIAA 2013-0780,2013
10. Alexander Kuzmin, “Sensitivity Analysis of Transonic Flow over J-78 Wings”, International Journal of Aerospace Engineering Volume 2015, Article ID 579343,2015
11. Dzianis PROSHCHANKA, Koichi YONEZAWA and Yoshinobu TSUJIMOTO, “Investigation of Three-Dimensional Unsteady Flow Characteristics in Transonic Diffusers”, Trans. JSASS Aerospace Tech. Japan Vol. 8, No. ists27, pp. Pe_53-Pe_59, 201
12. https://www.telegraph.co.uk/travel/travel-truths/which-passenger-jet-plane-flies-the-fastest/ (14-09-2019)
13. Islam, Asad. (2017). Verification and Validation of Flow over a 3D ONERA Wing using CFD Approach. Journal of Space Technology
14. https://www.grc.nasa.gov/www/wind/valid/m6wing/m6wing.html (14-09-2019)
15. Schmitt, V. and F. Charpin, "Pressure Distributions on the ONERA-M6-Wing at Transonic Mach Numbers," Experimental Data Base for Computer Program Assessment. Report of the Fluid Dynamics Panel Working Group 04, AGARD AR 138, May 1979.
16. http://jullio.pe.kr/fluent6.1/help/html/ug/node406.htm (26-06-2019)
17. NASA’s Glenn Research Center validation archive: Slater,John W., “ONERA M6 Wing Study #1.”ONERA M6 Wing. NPARC, n.d. Web.
18. Alexander Kuzmin, “Sensitivity Analysis of Transonic Flow ver J-78 Wings”, International Journal of Aerospace Engineering Volume 2015, Article ID 579343, 2015

NOMENCLATURE

Symbol	Meaning	Unit
C_D	Drag coefficient	Dimensionless
C_L	Lift Coefficient	Dimensionless
V	Velocity	m/s